SF2A 2023
M. N'Diaye, A. Siebert, N. Lagarde, O. Venot, K. Baillié, M. Béthermin, E. Lagadec, J. Malzac, J. Richard (eds)

FAR-IR POLARIZED EMISSION IN THE CRAB NEBULA WITH SOFIA/HAWC+

J. Chastenet[1], I. Looze[1,2], B. Hensley[3], B. Vandenbroucke[4], M. Barlow[2], J. Rho[5], A. Ravi[6], H. Gomez[7], F. Kirchschlager[1,2], J. Macías-Pérez[8], M. Matsuura[7], K. Pattle[2], N. Ponthieu[9], F. Priestley[7], M. Relaño[10,11], A. Ritacco[12,13] and R. Wesson[2]

Abstract. We present detection of dust polarized emission of the Crab Nebula (M 1) in the far-infrared, from SOFIA/HAWC+ observations, at 89 and 154 μm. After removing the signal from synchrotron emission, including its polarized component, we compute the average dust-only polarization in three dusty filaments, ranging from $\sim 3-9\%$. We constrain the grain temperatures and masses, assuming mixtures of silicate- and carbon-rich grains, using laboratory properties. Upper limits on the total dust mass in the Crab Nebula range from 0.027 to 1.0 $M_\odot$, and a fraction of carbon grains ranging from 0.2 to 70%.

Keywords: polarization, supernovae: individual: Crab, dust, emission, ISM: supernova remnants

This proceeding is an excerpt of the paper published by Chastenet et al. (2022). Please refer to the paper for more details.

1 Introduction

Supernovae (SNe) and supernova remnants (SNRs) affect the total dust budget of their host galaxy, be it in an effectively positive or negative sense. The formation of dust grains after these explosions could happen in the ejecta, thanks to the metal-rich environment that was birthed with the release of the elements formed in the progenitors (e.g., Barlow et al. 2010; De Looze et al. 2017; Chawner et al. 2020). But the shock waves sent out in the surrounding medium, that can rebound and run through the inner part of the SNR can be strong enough to fragment and destroy (newly) formed grains (e.g., Jones et al. 1994; Bocchio et al. 2016; Slavin et al. 2020; Kirchschlager et al. 2022).

The tensions between the observed and theoretical dust budget are often explained with the growth of dust grains in the dense interstellar medium (ISM), but this hypothesis comes with some caveats (e.g., Zhukovska et al. 2018; Galliano et al. 2021; Priestley et al. 2021). Another –or simultaneous– explanation could be that SNR destruction rates have been overestimated (e.g., Matsuura et al. 2009; Ferrara & Peroux 2021). These rates can vary depending on several parameters such as the size and composition (carbon- vs silicate-rich) of the considered grains, the energy released in the explosion, the density contrast of the dusty clumps where grains are found (e.g., Nozawa et al. 2007; Silvia et al. 2010; Micelotta et al. 2016; Kirchschlager et al. 2019).

[1] Sterrenkundig Observatorium, Ghent University, Krijgslaan 281-S9, B-9000 Gent, Belgium
[2] Dept. of Physics & Astronomy, University College London, Gower Street, London WC1E 6BT, UK
[3] Department of Astrophysical Sciences, Princeton University, Princeton, NJ 08544, USA
[4] Leiden Observatory, Leiden University, NL-2300 RA Leiden, Netherlands
[5] SETI Institute, 189 N. Bernardo Ave., Ste. 200, Mountain View, CA 94043
[6] Box 19059, Department of Physics, University of Texas at Arlington, Arlington, TX 76019, USA
[7] School of Physics and Astronomy, Cardiff University, Queens Buildings, The Parade, Cardiff CF24 3AA
[8] Univ. Grenoble Alpes, CNRS, Grenoble INP, LPSC-IN2P3, 53, avenue des Martyrs, 38000 Grenoble, France
[9] Univ. Grenoble Alpes, CNRS, IPAG, 38000 Grenoble, France
[10] Departamento Física Teórica y del Cosmos, Universidad de Granada, E-18071 Granada, Spain
[11] Instituto Universitario Carlos I de Física Teórica y Computacional, Universidad de Granada, E-18071 Granada, Spain
[12] INAF-Osservatorio Astronomico di Cagliari, Via della Scienza 5, 09047 Selargius, IT
[13] Laboratoire de Physique de l'École Normale Supérieure, ENS, PSL Research University, CNRS, Sorbonne Université, Université de Paris, 75005, Paris, France

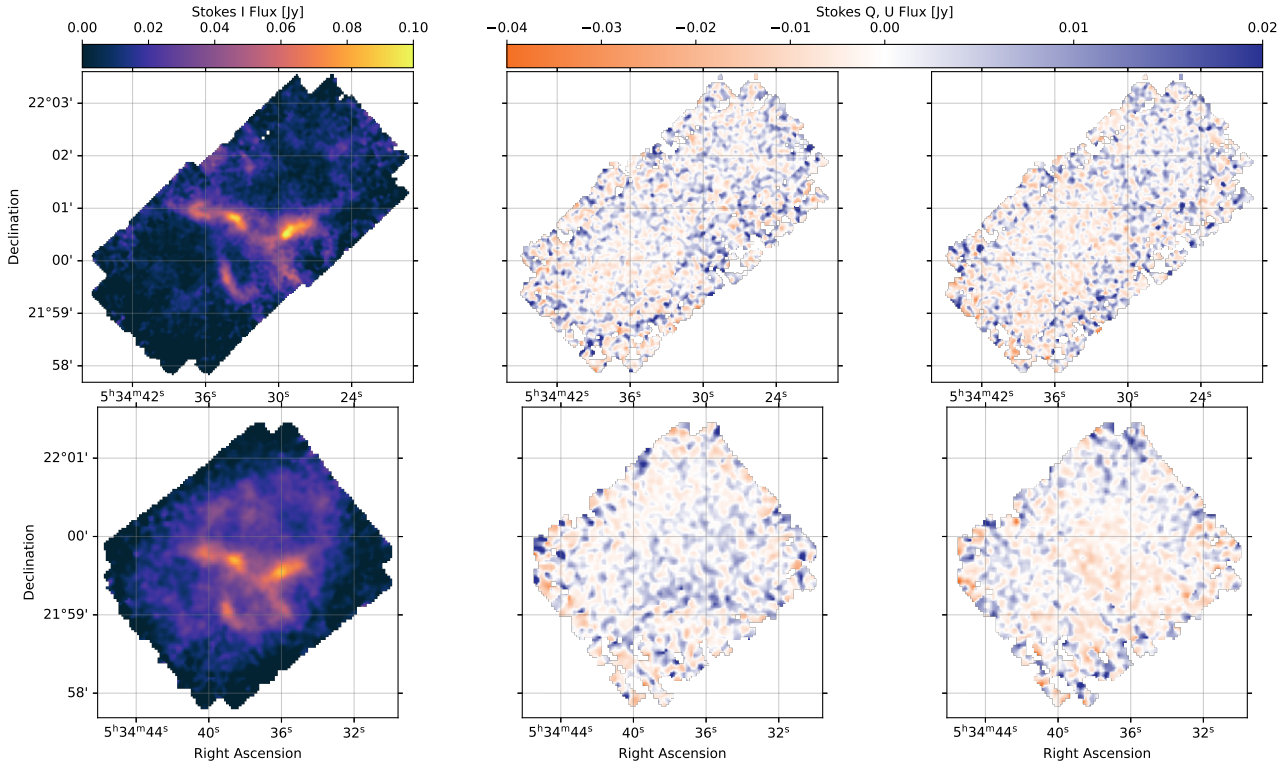

Fig. 1. *Left to right:* Stokes I, Q, and U parameters from SOFIA/HAWC+ observations in band C 89 μm (top) and band D 154 μm (bottom), at native resolutions, 7.8″ and 13.6″, respectively.

In this study, we use a new approach to constrain the mass, size, and composition of dust grains in a well-studied SNR, the Crab Nebula. Instead of performing spectral energy distribution fitting, we use polarization information and physical dust properties to derive grain temperatures and masses.

2 Data preparation and processing

2.1 New far-IR data, and radio synchrotron observations

The data was taken on September 2018 as part of the proposal 06_0193 (PI: De Looze). Observations were done in bands C (89 μm, FWHM $\sim$ 7.8″) and D (154 μm, FWHM $\sim$ 13.6″), using the HAWC+ instrument (Harper et al. 2018), on-board the Stratospheric Observatory for Infrared Astronomy (SOFIA; Temi et al. 2018) . We use the Level 4 data from the SOFIA pipeline for the Stokes vector (I, Q, U parameters), shown in Figure 1, but we calculate the debiased polarization using the modified asymptotic estimator as described in Plaszczynski et al. (2014). This allows a more robust estimate at low signal-to-noise ratios.

We use NIKA 150 GHz radio data (FWHM $\sim$ 18″) from Ritacco et al. (2018, , and reference therein) to estimate the synchrotron polarization parameters. We estimate the fraction of synchrotron emission in bands C and D from the results from De Looze et al. (2019), who fit a multi-component model to the infrared emission of the Crab. All their data products were estimated at the *Herschel*/SPIRE 500 resolution, which is $\sim$ 36″. We convolve and regrid our HAWC+ data to that same resolution.

2.2 Synchrotron radiation removal and dust-only polarization

The synchrotron radiation was shown to be significant in the Crab at far-IR wavelengths, between 20 and 35% by De Looze et al. (2019), and we need to remove it to focus on dust-only polarized emission. We use the NIKA radio data, where we consider that the measured emission is due to synchrotron radiation only, and estimate a synchrotron polarization fraction and angle. Assuming that the polarization fraction is constant

	$MgSiO_3$ amorphous	**$MgSiO_3$ glassy**	**Mg_2SiO_4**	**$Mg_{0.5}Fe_{0.5}SiO_3$**	**$Mg_{0.7}SiO_{2.7}$**
	Temperature [K]				
Silicates	$31.8 - 46.9$	$33 - 50$	$31.8 - 46.9$	31.45.1	33.450.9
Carbonaceous	$39 - 67.7$	$38.8 - 67.1$	$38.9 - 67.5$	$38.8 - 67$	$38.8 - 67$
	Total dust mass, upper limits [$M_\odot$]				
Estimate 1	$0.040 - 0.059$	$0.026 - 0.032$	$0.037 - 0.054$	$0.27 - 0.53$	$0.027 - 0.34$
Estimate 2	0.11	0.061	0.10	1.0	0.065
	f_{aC} [%]				
	$6 - 50$	$17 - 70$	$9 - 53$	$0.2 - 8$	$17 - 68$

Table 1. Dust grain temperatures, upper-limits on total dust mass in the Crab, and estimated fraction of carbon-rich grains for 5 types of silicate-rich grains. The ranges shown here cover all three ellipses encompassing dusty filaments, and the dust masses range additionally covers results for a range of zenith angle $45^\circ \leq \theta \leq 90^\circ$.

across wavelengths, we use the work from De Looze et al. (2019) to estimate the synchrotron contamination at the HAWC+ wavelengths, in all Stokes parameters.

3 Constraining dust properties

Given the only two accessible polarized measurements at 89 and 154 μm, we do not perform spectral energy distribution fitting. Instead, we proceed to constrain dust grain temperatures and masses step by step. Because of the limited number of data points, we are forced to make a number of assumptions to simplify the system of equations. We assume that

- the dust is a mixture of silicate- and carbon-rich grains;
- both grain species have the same size distribution, with radius ranging 0.1 μm $\leq$ a $\leq$ 5.0 μm, and an ellipsoid-shape distribution;
- carbon grains do not align with the magnetic field and do not produce polarized signal;
- all silicate-rich grains align with the same angle (0.1 μm being the lower limit for efficient alignment);
- grains have reached an equilibrium temperature and follow the blackbody emission.

We derive grain emissivities using laboratory measurements of the (n, k) refractive indices, and the simulation code COSTUUM (Vandenbroucke et al. 2020). We test 5 different silicate-rich species: $MgSiO_3$, amorphous and glassy, Mg_2SiO_4, $Mg_{0.5}Fe_{0.5}SiO_3$, and $Mg_{0.7}SiO_{2.7}$. The carbon material is assumed to be that discussed in the optECs model (Jones 2012a,b,c).

We first derive silicate grain temperature using the ratio of polarized emission between bands C and D, and assuming a blackbody emission. We then solve for the carbon grain temperature, by using the ratio of polarization fractions between bands C and D. Using these temperatures and the observations, we derive the dust surface density for each component, and the corresponding fraction of carbon grains. We tabulate these results in Table 1. We only show an extract of the results, covering variations between each dusty filament, and for varying zenith angle (one of the assumptions needed to simplify the equations).

We extrapolate the derived dust masses to estimate upper-limits on the total dust mass in the Crab using two methods: (i) scaling the total dust mass within the three ellipses, to the area of the ellipse in De Looze et al. (2019), and (ii) scaling the highest dust mass in the ellipse to the area of the ellipse in De Looze et al. (2019). By construction Estimate 2 in Table 1 is the highest, and very conservative.

4 Conclusions

With SOFIA/HAWC+ observations, we present detection of far-IR dust polarization in the Crab nebula, second confirmed detection in a SNR after Cassiopeia A. Using polarized emission at 89 and 154 μ, and after removing contamination from synchrotron polarization using radio data, we measure the (integrated) polarization fractions and angles in three dusty filaments, at the SPIRE 500 resolution (36″). We assume a mixture of silicate- and carbon-rich grains and using laboratory refractory indices, and solve a system of equations instead of fitting spectral energy distributions to derive dust grain temperatures, masses, and fraction of carbon grains. We find

that large grains ($a > 0.1$ μm in radius) must be present in the Crab Nebula, and that carbon- and silicate-rich species likely co-exist in this SNR.

JC acknowledges support from ERC starting grant #851622 DustOrigin. This research is based on observations made with the NASA/DLR Stratospheric Observatory for Infrared Astronomy (SOFIA). SOFIA is jointly operated by the Universities Space Research Association, Inc. (USRA), under NASA contract NNA17BF53C, and the Deutsches SOFIA Institut (DSI) under DLR contract 50 OK 0901 to the University of Stuttgart.

References

Barlow, M. J., Krause, O., Swinyard, B. M., et al. 2010, A&A, 518, L138
Bocchio, M., Marassi, S., Schneider, R., et al. 2016, A&A, 587, A157
Chastenet, J., De Looze, I., Hensley, B. S., et al. 2022, MNRAS, 516, 4229
Chawner, H., Gomez, H. L., Matsuura, M., et al. 2020, MNRAS, 493, 2706
De Looze, I., Barlow, M. J., Bandiera, R., et al. 2019, MNRAS, 488, 164
De Looze, I., Barlow, M. J., Swinyard, B. M., et al. 2017, MNRAS, 465, 3309
Ferrara, A. & Peroux, C. 2021, MNRAS, 503, 4537
Galliano, F., Nersesian, A., Bianchi, S., et al. 2021, A&A, 649, A18
Harper, D. A., Runyan, M. C., Dowell, C. D., et al. 2018, Journal of Astronomical Instrumentation, 7, 1840008
Jones, A. P. 2012a, A&A, 540, A1
Jones, A. P. 2012b, A&A, 540, A2
Jones, A. P. 2012c, A&A, 542, A98
Jones, A. P., Tielens, A. G. G. M., Hollenbach, D. J., & McKee, C. F. 1994, ApJ, 433, 797
Kirchschlager, F., Mattsson, L., & Gent, F. A. 2022, MNRAS, 509, 3218
Kirchschlager, F., Schmidt, F. D., Barlow, M. J., et al. 2019, MNRAS, 489, 4465
Matsuura, M., Barlow, M. J., Zijlstra, A. A., et al. 2009, MNRAS, 396, 918
Micelotta, E. R., Dwek, E., & Slavin, J. D. 2016, A&A, 590, A65
Nozawa, T., Kozasa, T., Habe, A., et al. 2007, ApJ, 666, 955
Plaszczynski, S., Montier, L., Levrier, F., & Tristram, M. 2014, MNRAS, 439, 4048
Priestley, F. D., De Looze, I., & Barlow, M. J. 2021, MNRAS, 502, 2438
Ritacco, A., Macías-Pérez, J. F., Ponthieu, N., et al. 2018, A&A, 616, A35
Silvia, D. W., Smith, B. D., & Shull, J. M. 2010, ApJ, 715, 1575
Slavin, J. D., Dwek, E., Mac Low, M.-M., & Hill, A. S. 2020, ApJ, 902, 135
Temi, P., Hoffman, D., Ennico, K., & Le, J. 2018, Journal of Astronomical Instrumentation, 7, 1840011
Vandenbroucke, B., Baes, M., & Camps, P. 2020, AJ, 160, 55
Zhukovska, S., Henning, T., & Dobbs, C. 2018, ApJ, 857, 94